Inorganica Chimica Acta 421 (2014) 446–450

Contents lists available at ScienceDirect

Inorganica Chimica Acta

journal homepage: www.elsevier.com/locate/ica

Catalytic performance and mechanism of Cu(II)-hydrazone complexes as models of galactose oxidase

Huatian Shi, Yegao Yin *

Department of Chemistry, Shantou University, 243 University Road, Shantou 515063, China

ARTICLE INFO

Article history:
Received 7 March 2014
Received in revised form 12 June 2014
Accepted 20 June 2014
Available online 9 July 2014

Keywords:
Galactose oxidase
Copper(II)
Benzyl aldehyde
Catalysis mechanism
Model

ABSTRACT

As simulants of galactose oxidase (GO), three mononuclear Cu(II) complexes with 1-((3-*t*-Bu,5-R1)-salicylidenehydrazono),2-((3-*t*-Bu,5-R2)-salicylidenehydrazono)-1,2-diphenylethane ($H_2L^{Bu,Bu}$: R1 = R2 = *t*-butyl; $H_2L^{MeO,MeO}$: R1 = R2 = methoxyl; $H_2L^{Bu,MeO}$: R1 = *t*-butyl, R2 = methoxyl) as ligands were synthesized. X-ray diffraction defined their structures, like GO, all having a distorted square N_2O_2-coordinated Cu(II) center, and catalytic experiments confirmed their abilities to enable the aerobic oxidation of benzyl alcohol to benzaldehyde under room temperature with turnover numbers up to 823–1036. Voltammetric measurements indicated that the cupric phenolates are electroactive, in the range of 0.3–0.9 V (vs $E_{Fc+/Fc}$), all giving two anodic peaks symbolizing the formation of +1 and +2 charged complex radicals. The presence of radicals was proven by the thianthrene perchlorate titration UV–Vis spectra of **1**–**3** with showing two new absorptions typical for phenoxy radicals and by the electronic spin resonance spectra with revealing an antiferromagnetic coupling of phenoxy radicals with Cu(II) ($s = 1/2$).

1. Introduction

Molecularly modeling the metalloproteins that catalyze certain biochemical processes is one of the major interests of modern coordination chemistry [1–7]. Of aim to rationally design the model systems, a hard effort has focused on understanding the catalytic mechanism of metalloproteins, the correlation between the structures and properties of mimics and their operation mechanism [8–13]. Such being the case of GO, after an intensive investigation of their structure, spectroscopy and catalytic process [14–19], their phenoxyl radical-involving mechanism has been well understood [20], which has led to the emergence of a large sum of phenolate-coordinated Cu(II) complexes to stimulate the active site and function of GO [21–28]. As highlight of this topical research, Pierre, Stack and Halcrow have tactfully used salicylaldehyde Schiff bases to mimic the proteinic environment of Cu(II) in GO, thereby revealing that the mimics operation through providing the phenoxyl radicals of virtue intermediating the hydrogen abstraction [24–37] and that the performance of model complexes is subject to the phenol substitution [31–34].

As another probe to the effect of varied phenol substitution and extended π-conjugation of ligands on the function of such mimics, we prepared three complexes, namely [Cu(II)($L^{Bu,Bu}$)] (**1**), [Cu(II)($L^{MeO,MeO}$)] (**2**) and [Cu(II)($L^{Bu,MeO}$)] (**3**), of the ligands discriminated by 5,5′-substitution of salicylaldehyde, and investigated their catalytic performance and their responses to oxidative conditions. The results show that the complexes catalyze the aerobic oxidation of benzyl alcohol under solventless and room temperature conditions through a nucleophilic hydrogen abstraction.

2. Experiment

2.1. Materials and methods

2.1.1. General information

The chemicals, including 3,5-di-*tert*-butylsalicylaldehyde, and solvents used were available commercially. Oxidant, thianthrene perchlorate ($ThClO_4$) was prepared by a literature method [38]. To a mixed liquid of $HClO_4$ (0.8 ml) and acetic anhydride (50 ml) was added a CCl_4 solution (100 ml) of thianthrene (0.5 g, 0.046 mol). The solution was stood overnight and then gave the crystals of $ThClO_4$. The product was collected by filtration, followed by washing with CCl_4 and drying in vacuum, in yield *ca* 90% (UV–Vis absorption in CH_2Cl_2: $\lambda_{max} = 550$ nm, $\varepsilon = 8500\ M^{-1}\ cm^{-1}$).

2.1.2. Single crystal determination

The single crystals of **1**–**3** for structural analyses were obtained from evaporating the reaction solutions of ligands and $CuCl_2{\cdot}4H_2O$ in ethanol. Single-crystal X-ray diffraction data for **1**–**3** were

* Corresponding author.
E-mail address: ygyin@stu.edu.cn (Y. Yin).

http://dx.doi.org/10.1016/j.ica.2014.06.031
0020-1693/

collected on an Agilent Technologies Gemini A System (Mo Kα, λ = 0.710 73 Å) at 298 K. The data were processed using CrysAlis-Pro.1 and corrected and scaled using the SCALE3 ABSPACK scaling algorithm. The structures of **1**–**3** were solved by direct method [39] and refined by a least-square fitting method using Olex 2 Program [40].

2.1.3. Cyclic voltammetry

The electrochemical measurements were performed on a Zahner Im6ex system with a standard three-electrode cell, consisting of a platinum disk as working electrode, a platinum wire as auxiliary and a Ag/AgCl as reference. The samples were made of 1.0×10^{-3} M CH_2Cl_2 solutions with adding 0.1 M $(n\text{-Bu})_4NPF_6$ as supporting electrolyte. The potentials were recorded in reference to $E_{1/2(\text{ferrocenium/ferrocene})}$ (shortened for $E_{Fc+/Fc}$) in a scan rate 100 mV/s.

2.1.4. EPR spectroscopy

Electron paramagnetic resonance (EPR) spectra were determined on a Bruker EMX spectrometer at 293 K using 1×10^{-3} M CH_2Cl_2 solutions of samples. The frequency of microwave was kept at 9.810511 GHz, the illuminated energy at 20 mW and the scan range as 1000 G – 5000 G. Spin quantitation was carried out by double integration of derivative EPR spectra and normalized to the intensity before the addition of 1 eq $ThClO_4$.

2.1.5. UV–Vis spectroscopy

The titration UV–Vis spectra of **1**–**3** were recorded on a Perkin Elmer Lambda 950 UV–Vis Spectrometer by each time adding 30 μl of saturated $ThClO_4$ solution until twice the equivalent of complexes.

2.1.6. Catalytic performance

The catalytic performance experiments were performed in the Schlenk-flask under pure O_2 sphere. NaOH (0.2 g) was dissolved into Benzyl alcohol (20 ml) before the addition of complex (2 mg). The blank experiment was assembled the same above except without adding the complex. The mixture resulted with O_2 bubbling and stirring in 20 h was analysed by a Shimadzu GC–MS spectrometer and the production of benzyl aldehyde was determined on a Anglient 1100 series HPLC equipment using the detecting wavelength at 248 nm, with mobile phases CH_3CN:H_2O = 45:55. The results are the average of three runs.

2.2. Synthesis of ligands and complexes

2.2.1. Synthesis of 3-tert-butyl-5-methoxylsalicylaldehyde

The intermediate was prepared by a known method [41]. A mixture of 3-*tert*-butyl-4-hydroxyanisole (7.35 g, 40 mmol) and urotropine (11.25 g, 80 mmol) in glacial acetic acid (40 ml) was heated at 110 °C for 2 h. After disappearance of 3-*tert*-butyl-4-hydroxyanisole, a H_2SO_4 solution (33%, 40 ml) was added to it at 75 °C. The resulting mixture was heated again at 110 °C for another 3 h and then was extracted with 100 ml of diethyl ether. The extract was washed with two portions of 100 ml water, then two portions of 100 ml saturated Na_2CO_3 solution and finally 100 ml saturated NaCl solution. The organic layer was dried over $MgSO_4$, and then the solvent was removed by evaporation under a reduced pressure. The residue dissolved in CH_2Cl_2 (10 ml) was passed through a silica column using CH_2Cl_2 as eluent to give the aldehyde as yellow oil in yield of about 60% (5 g).

2.2.2. Synthesis of benzyl dihydrazone

The intermediate was harvested as white precipitates from refluxing the ethanolic solution (100 ml) of enzyl (10.5 g, 0.05 mol) and excessive hydrazine (20 ml, 80%) for 6 h. With recrystallizing the precipitates in ethanol, white needle crystals as dihydrazone were collected in yield of 60% (8 g).

2.2.3. Synthesis of $H_2L^{Bu,Bu}$ and $H_2L^{MeO,MeO}$

The symmetric ligands were prepared in parallel with refluxing the mixture of dihydrazone (1.19 g, 0.005 mol) and 2 eqs of corresponding substituted salicylaldehydes in 100 ml alcohol for 6 h. For $H_2L^{Bu,Bu}$, the dosage of aldehyde is 2.34 g (0.01 mol) and the yield is 80% (3 g). ^{1}HNMR (400 MHz, $CDCl_3$): δ 11.24 (s, 2H, OH), 8.73 (s, 2H, CH = N), 7.90 (m, 4H, ArH), 7.43 (m, 6H, ArH), 7.33 (d, J = 2.4 Hz, 2H, ArH), 7.07 (d, J = 2.4 Hz, 2H, ArH), 1.32 (s, 18H, 3-$C(CH_3)_3$), 1.25 (s, 18H, 5-$C(CH_3)_3$), and, for $H_2L^{MeO,MeO}$, the amount of aldehyde is 2.08 g (0.01 mol) and the yield is 88% (3 g). ^{1}H NMR (400 MHz, $CDCl_3$) δ 11.04 (s, 2H, –OH), 8.68 (s, 2H, N=CH), 7.96–7.81 (m, 4H, ArH), 7.52–7.34 (m, 6H, ArH), 6.92 (d, J = 3.0 Hz, 2H,ArH), 6.57 (d, J = 3.0 Hz, 2H, ArH), 3.72 (s, 6H, –OCH_3), 1.27 (s, 18H, $C(CH_3)_3$).

2.2.4. Synthesis of ligand $H_2L^{Bu,MeO}$

The asymmetric ligand was prepared by first dropwise adding the ethanol solution (100 ml) of 3,5-di-*tert*-butyl-2-hydroxylphenzyl aldehyde (1.17 g, 0.005 mol) into a solution (20 ml) of enzyl dihydrazone (1.19 g, 0.005 mol) at ambient temperature under stirring within 2 hs, and then a solution (10 ml) of 3-*tert*-butyl-5-methoxylsalicylaldehyde (1.04 g, 0.005 mol). After that, the solution was refluxed for another 2 h and then cooled down to room temperature. Evaporation of the solution gave the yellow solids of $H_2L^{Bu,MeO}$ in yield of 77%. ^{1}H NMR (400 MHz, $CDCl_3$) δ 11.23 (s, 1H, –OH), 11.05 (s, 1H, –OH), 8.73 (s, 1H, CH=N), 8.68 (s, 1H, CH=N), 7.93–7.87 (m, 4H, ArH), 7.49–7.37 (m, 6H, ArH), 7.33 (d, J = 2.4 Hz, 1H, ArH), 7.07 (d, J = 2.4 Hz, 1H, ArH), 6.92 (d, J = 3.0 Hz, 1H,ArH), 6.57 (d, J = 3.0 Hz, 1H, ArH), 3.72 (s, 3H, –OCH_3), 1.32 (s, 9H, $C(CH_3)_3$), 1.30 (s, 9H, $C(CH_3)_3$), 1.25 (s, 9H, $C(CH_3)_3$).

*2.2.5. Syntheses ef model compounds **1**–**3***

These complexes were synthesized similarly as follows: To an alcoholic solution (25 ml) of ligand (0.1 mmol) and NaOH (0.2 mmol) was added solution (5 ml) of $CuCl_2{\cdot}2H_2O$ (0.02 g, 0.2 mmol). The mixed solution was heated to boil and then cooled down to room temperature. The solution was evaporated in room for about 2 days and then gave the black block crystals of complex. **1** (ESI-MS(M+1): 732. *Anal.* Calc. C, 72.131; N, 7.650; H, 7.104. Found: C, 71. 93; N, 7.65; H, 7.42%) in yield of 95% (0.07 g) based on amount of ligand. **2** (ESI-MS(M+1): 680. *Anal.* Calc. C, 67.059; N, 8.235; H, 5.882. Found: C, 66.87; N, 8.19; H, 6.176%) in yield of 88% (0.06 g) and **3** (ESI-MS(M+1): 706. *Anal.* Calc. C, 69.688; N, 7.932; H, 6.516. Found: C, 69.72; N, 8.16; H, 6.579%) in yield of 89% (0.063 g).

3. Results and discussion

*3.1. Structures and catalytic performance of **1**–**3***

X-ray diffraction defined the structures of **1**–**3** as the mononuclear complexes crystallizing in a monoclinic $\mathbf{P}2_1/c$ space group (Table S1). Fig. 1 specifies their assembly, indicating that the mimics, like GO [20], all have a N_2O_2-coordinated Cu(II) center, and, owing to the repulsion between the phenyls of enzyl, their coordination centers are obviously distorted from a planar square. Of note is that, despite the alteration of R1 and R2, the metal-involving bond facts of **1**–**3** are not drastically different (Table S2), in a way, rationalizing the ascription of the function diversity of **1**–**3** to the effect of substitution. Moreover, it is noticed that the obtuse N–Cu–O angles of **1**–**3**, as those of salen-type mimics [28], are

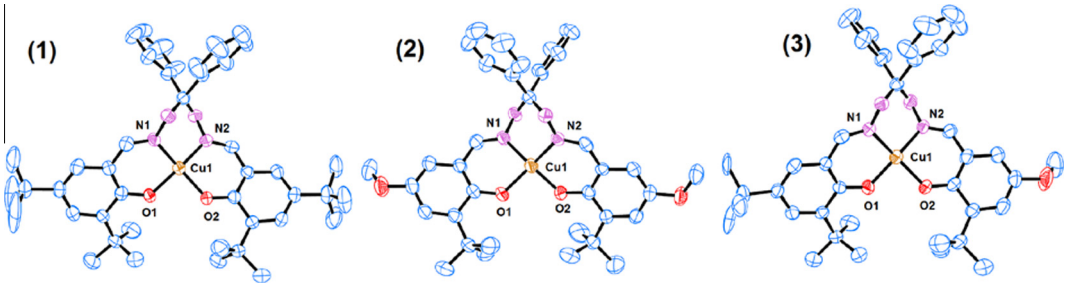

Fig. 1. The ORTEP drawings of **1**–**3** (from left to right) with hydrogen atoms omitted for clarity(Carbon: blue; Oxygen: red; Nitrogen: purple; Copper: brown). (For interpretation of the references to color in this figure legend, the reader is referred to the web version of this article.)

larger than 150°, and so we expect the Cu(II) sites to be open, allowing the attack of alcohol substrate.

On this consideration, we evaluated the catalytic activities of **1**–**3** by determining the yields of benzyl aldehyde from bubbling benzyl alcohol containing 0.2 g NaOH with air in the presence of 2 mg complexes for 20 h. Chromatographic analysis verified that the catalyzed reactions are high yielding with turnover numbers as 823, 1036 and 979 (turnover frequency(TOF): 0.0114 s^{-1}, 0.0144 s^{-1}, 0.0136 s^{-1}), average data of three independent catalytic runs, and there is no any benzoic acid found in the blank and catalytic experiment, which means that no further oxidation of benzyl aldehyde happens in the system. This result comparable with the reported [28], and so promises the application of **1**–**3** as catalysts for aerobic oxidation of benzyl alcohol in solventless and room temperature conditions.

3.2. Responses of *1*–*3* to oxidative conditions

It is well known that Cu(II)-phenolate systems are electroactive [42]. To have an insight into the responses of **1**–**3** to aerobic condition ($E_{O2/OH-}$ = 0.61 V versus $E_{Fc+/Fc}$), we examined their redox behavior in the range of −0.5–1.0 V, thereby obtaining the voltammograms shown in Fig. 2, which revealed a variety of these model compounds in oxidation propensity. It is easily seen that the plots of **1** and **2** are similarly exhibiting two quasi-reversible redox pairs, which can be assigned to the processes [CuL] ↔ $[CuL^{*}]^{+}$ ↔ $[CuL^{**}]^{2+}$ [26,27,32]. However, a scrutiny reveals that the E^{1}_{pa} of **2** is less positive than that of **1**, so meaning an easier formation of $[2^{*}]^{+}$ than $[1^{*}]^{+}$, and the separation ΔE_{pa} ($E^{2}_{pa} - E^{1}_{pa}$) of **2** is smaller (the detailed information is presented in Table S3), indicating a less stability of $[2^{*}]^{+}$ (the disproportionation constant *Kc* for $[1^{*}]^{+}$ is 1.43×10^{5}, for $[2^{*}]^{+}$ is 3.95×10^{4}). Logically, the easier formation and less stability of $[2^{*}]^{+}$ are stemmed in the effect of more electron-donating of MeO because it enriches the electron on phenolates. This is agreed by the CV curve of **3** with giving an E^{1}_{pa}, relating to oxidation of MeO substituted phenolate, close to that of **2**, and a E^{2}_{pa}, relating to oxidation of butylated phenolate, close to that of **1** [33,43]. This pattern also comes to a conclusion that these oxidations are ligand-base [33].

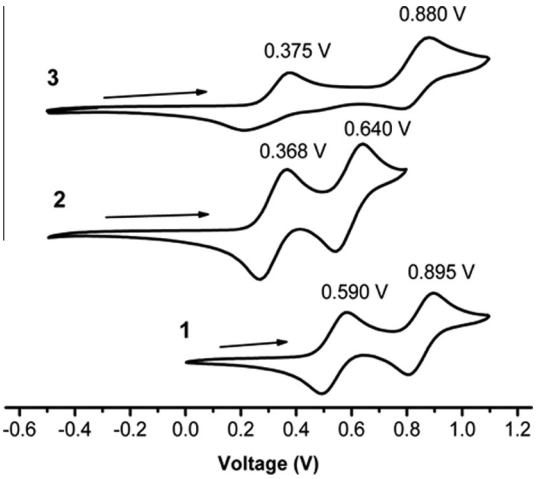

Fig. 2. The voltammograms of **1**–**3** with the peak potentials recorded in reference to $E_{Fc+/Fc}$.

Associating the electrochemical readings to the catalytic efficiencies of **1**–**3**, we come to an conclusion that the activities of the model compounds are subject to the substitution of phenol, or saying, an electron enrichment on phenol benefits the catalysis of complexes [31]. The conclusion implicates that the hydrogen abstraction of benzalcohol is actually a nucleophilic process. This is supported by the fact that the tyrosyl radicals in photosystem II and ribonucleotide reductase are hydrogen-bonded to acidic residues [44,45]. Also, it is noticeable that the hydrazone adducts, compared with those of the non-conjugating salen-type ligands, are less oxidizable with the E^{1}_{pa} more positive [22,32]. To this observation, a possible account is that extended conjugation of ligands disperses the electrons on phenol oxygen by *p*–π conjugation, which has been proved by the comparison of the oxidation potentials of Schiff bases of saturated [22,32,33] and unsaturated diamines [27,32]. In this sense, an extended conjugation of ligand makes the formation of univalent radicals difficult, and hence lowers the activity of complexes.

As evidence of the presence of phenoxy radicals under oxidative condition, we examined the change of UV–Vis spectra of **1**–**3** with titration by $ThClO_4$ ($E_{1/2}$ = 0.89 V versus $E_{Fc+/Fc}$) [46], an oxidant that expectedly can bring the production of cationic radicals (Scheme 1). Fig. 3 gives the spectra before addition (more details are presented in Table S4), indicating that the complexes are akin showing the bands arising from intraligand charge transfer (ILCT) in the range of 250–300 nm, from ligand–metal change transfer (LMCT) near 450 nm and from *d*–*d* transition at *ca* 670 nm [47]. Of the bands, LMCT is most diagnostic of the effect of substitution since its energy is directly relating to the electronic affinity of ligand [48]. This is proven true by the LMCT of **1** with highest energy relating to weak electron-donation of *t*-Bu, of **2** with a lowest energy to strong donation of MeO, and of **3** covering the peaks of **1** and **2** to symbolize both the two transitions.

As represented by the spectra of **2** (Fig. 4) (those of **1** and **3** are given in Fig. S1), with adding $ThClO_4$ the LMCTs of **1**–**3** decrease gradually and meanwhile the new bands attributable to the absorptions of +1 charged radicals [49–54], are formed in the range

$$[CuL] + [Th^{*}]^{+}ClO_4^{-} \longrightarrow [CuL^{*}]^{+}ClO_4^{-} + Th$$

$$[CuL^{*}]^{+}ClO_4^{-} + [Th^{*}]^{+}ClO_4^{-} \longrightarrow [CuL^{**}]^{2+}(ClO_4^{-})_2 + Th$$

Scheme 1. The possible reactions of **1**–**3** (generally denoted as [CuL]) titrated by $ThClO_4$.

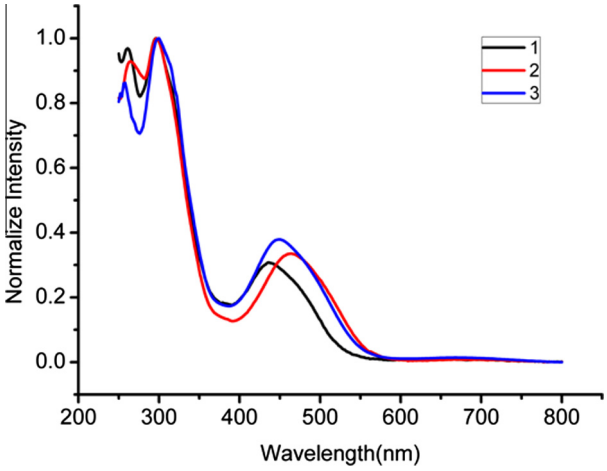

Fig. 3. The UV–Vis absorption spectra of **1**–**3** in dichloromethane.

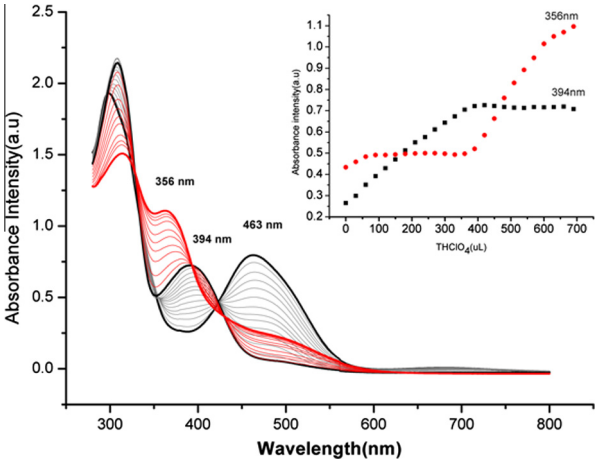

Fig. 4. UV–Vis spectra of **2** titrated by $ThClO_4$ (0–2 equivalents); the insert shows the intensity changes of 394 nm relating to $[2^*]^+$ and 356 nm relating to $[2^{**}]^{2+}$ with adding $ThClO_4$.

of 350–400 nm, and, as adding more than equimolar $ThClO_4$, the new bands diminished and, simultaneously, the bands symbolizing the formation of +2 charged radicals appeared in the higher energy region. The observations suggest strongly that, under aerobic condition, the complexes could produce +1 phenoxyl radicals that could intermediate the hydrogen abstraction [28,32].

3.3. Magnetical responses of *1*–*3* to oxidation

As additional proof of the presence of +1 charged radicals, the EPR spectra of **1**–**3** were determined before and after adding equimolar $ThClO_4$. As seen in Fig. S2, the spectra of **1**–**3** give the anisotropic signals centered at $g = 2.04$, 2.08 and 2.11, typical for a distorted planar coordination of Cu(II) [55]. The magnetic responses of **1**–**3** are similar to those of reported models [26–35] and that of GO [20], and thus confirm the fine imitation of models. But, with adding equimolar $ThClO_4$, the EPR signals show varied degrees of intensity decreases, due to the delocalization of some spin density on the phenzyl ring [34], indicating an antiferromagnetic interaction between phenoxyl radicals and Cu(II) ion [56].

4. Conclusion

In brief, the work reports a new Cu(II)-hydrazone model system of GO. Catalysis experiments confirmed the abilities of **1**–**3** to catalyze the aerobic oxidation of benzyl alcohol to benzaldehyde under solventless and ambient temperature conditions. Combined electrochemical, spectroscopic and magnetochemical investigations proved their catalytic mechanism through providing monophenoxy radicals as Lewis bases to intermediating hydrogen abstraction.

Notes

The authors declare no competing financial interest.

Acknowledgements

This work is financially supported by the National Natural Science Foundation (20971083) and the Natural Science Foundation of Guangdong Province (9151503101000629).

Appendix A. Supplementary material

CCDC 990098–990100 contains the supplementary crystallographic data for **1**–**3**. These data can be obtained free of charge from The Cambridge Crystallographic Data Centre via www.ccdc.cam.ac.uk/data_request/cif. Supplementary data associated with this article can be found, in the online version, at http://dx.doi.org/10.1016/j.ica.2014.06.031.

References

[1] R.M. Roat-Malone, Bioinorganic Chemistry: A Short Course, John Wiley & Sons Inc, 2007.
[2] B.A. MacKay, M.D. Fryzuk, Chem. Rev. 104 (2004) 385.
[3] E.Y. Tshuva, S.J. Lippard, Chem. Rev. 104 (2004) 987.
[4] L.M. Mirica, X. Ottenwaelder, T.D.P. Stack, Chem. Rev. 104 (2004) 1013.
[5] S. Mukhopadhyay, S.K. Mandal, S. Bhaduri, W.H. Armstrong, Chem. Rev. 104 (2004) 3981.
[6] E. Kim, E.E. Chufán, K. Kamaraj, K.D. Karlin, Chem. Rev. 104 (2004) 1077.
[7] K.C. MacLeod, P.L. Holland, Nat. Chem. 5 (2013) 559.
[8] E.I. Solomon, T.C. Brunold, M.I. Davis, J.N. Kemsley, S.K. Lee, N. Lehnert, J. Zhou, Chem. Rev. 100 (2000) 235.
[9] M.H. Baik, M. Newcomb, R.A. Friesner, S. Lippard, J. Chem. Rev. 103 (2003) 2385.
[10] B.K. Burgess, D.J. Lowe, Chem. Rev. 96 (1996) 2983.
[11] S. Shaik, S. Cohen, Y. Wang, H. Chen, D. Kumar, W. Thiel, Chem. Rev. 110 (2010) 949.
[12] S. Shaik, H. Chen, D. Janardanan, Nat. Chem. 3 (2010) 19.
[13] K.M. Lancaster, M. Roemelt, P. Ettenhuber, Y. Hu, M.W. Ribbe, F. Neese, S. DeBeer, Science 334 (2011) 974.
[14] N. Ito, S. Phillips, J. Mol. Biol. 238 (1994) 794.
[15] M.S. Rogers, D.M. Dooley, Curr. Opin. Chem. Biol. 7 (2003) 189.
[16] S.J. Firbank, M.S. Rogers, C.M. Wilmot, D.M. Dooley, M.A. Halcrow, P.F. Knowles, M.J. McPherson, S.E.V. Phillips, PNAS 98 (2001) 12932.
[17] M.S. Rogers, E.M. Tyler, N. Akyumani, C.R. Kurtis, R.K. Spooner, S.E. Deacon, S. Tamber, S.J. Firbank, K. Mahmoud, P.F. Knowles, S.E.V. Phillips, M.J. McPherson, D.M. Dooley, Biochemistry 46 (2007) 4606.
[18] C. Wright, A.G. Sykes, J. Inorg. Biochem. 85 (2001) 237.
[19] Y.K. Lee, M.M. Whittaker, J.W. Whittaker, Biochemistry 47 (2008) 6637.
[20] J.W. Whittaker, Chem. Rev. 103 (2003) 2347.
[21] S. Itoh, M. Taki, S. Takayama, S. Nagatomo, T. Kitagawa, N. Sakurada, S. Fukuzumi, Angew. Chem., Int. Ed. 38 (1999) 2774.
[22] E. Saint-Aman, J.L. Pierre, E. Defrancq, G. Gellon, New J. Chem. 22 (1998) 393.
[23] P. Chaudhuri, M. Hess, U. Flörke, K. Wieghardt, Angew. Chem., Int. Ed. 37 (1998) 2217.
[24] N. Kitajima, K. Whang, Y. Moro-oka, A. Uchida, Y. Sasada, J. Chem. Soc., Chem. Commun. (1986) 1504.
[25] P. Chaudhuri, M. Hess, T. Weyhermüller, K. Wieghardt, Angew. Chem., Int. Ed. 38 (1095–109) (1999) 8.
[26] P. Chaudhuri, M. Hess, J. Müller, K. Hildenbrand, E. Bill, T. Weyhermüller, K. Wieghardt, J. Am. Chem. Soc. 121 (1999) 9599.
[27] Y. Wang, T.D.P. Stack, J. Am. Chem. Soc. 118 (1996) 13097.
[28] Y. Wang, J.L. DuBois, B. Hedman, K.O. Hodgson, T.D.P. Stack, Science 279 (1998) 537.
[29] F. Thomas, O. Jarjayes, C. Duboc, C. Philouze, E. Saint-Aman, J.L. Pierre, Dalton Trans. 17 (2004) 2662.
[30] I. Sylvestre, J. Wolowska, C.A. Kilner, E.J. McInnes, M.A. Halcrow, Dalton Trans. (2005) 3241.
[31] V.B. Arion, S. Platzer, P. Rapta, P. Machata, M. Breza, D. Vegh, A. Pombeiro, J. Inorg. Chem. 52 (2013) 7524.

[32] R.C. Pratt, T.D.P. Stack, J. Am. Chem. Soc. 125 (2003) 8716.
[33] R.C. Pratt, C.T. Lyons, E.C. Wasinger, T.D.P. Stack, J. Am. Chem. Soc. 134 (2012) 7367.
[34] P. Verma, R.C. Pratt, T. Storr, E.C. Wasinger, T.D.P. Stack, PNAS 108 (2011) 18600.
[35] K. Asami, K. Tsukidate, S. Iwatsuki, F. Tani, S. Karasawa, L. Chiang, Y. Shimazaki, Inorg. Chem. 51 (2012) 12450.
[36] M. Orio, O. Jarjayes, H. Kanso, C. Philouze, F. Neese, F. Thomas, Angew. Chem., Int. Ed. 49 (2010) 4989.
[37] M.A. Halcrow, L.M.L. Chi, X. Liu, E.J.L. McInnes, L.J. Yellowlees, F.E. Mabbs, I.J. Scowen, M. McPartlin, J.E. Davies, J. Chem. Soc., Dalton Trans. (1999) 1753.
[38] Y. Murata, H.J. Shine, J. Org. Chem. 34 (1969) 3368.
[39] G.M. Sheldrick, Acta Crystallogr., Sect. A 64 (2008) 112.
[40] O.V. Dolomanov, L.J. Bourhis, R.J. Gildea, J.A.K. Howard, H. Puschmann, J. Appl. Crystallogr. 42 (2009) 339.
[41] J.F. Larrow, E.N. Jacobsen, Y. Gao, Y. Hong, X. Nie, C.M. Zepp, J. Org. Chem. 59 (1994) 1939.
[42] P. Chaudhuri, K. Wieghardt, Prog. Inorg. Chem. 50 (2001) 151.
[43] T. Kurahashi, H. Fujii, J. Am. Chem. Soc. 133 (2011) 8307.
[44] Y. Umena, K. Kawakami, J.R. Shen, N. Kamiya, Nature 473 (2011) 55.
[45] J. Stubbe, D.G. Nocera, C.S. Yee, M.C. Chang, Chem. Rev. 103 (2003) 2167.
[46] N.G. Connelly, W.E. Geiger, Chem. Rev. 96 (1996) 877.
[47] F. Thomas, Eur. J. Inorg. Chem. (2007) 2379.
[48] J.S. Griffith, The Theory of Transition-Metal Ions, Cambridge University Press, 1961.
[49] E.J. Land, G. Porter, E. Strachan, Trans. Faraday Soc. 57 (1961) 1885.
[50] E.J. Land, G. Porter, Trans. Faraday Soc. 59 (1963) 2016.
[51] L.I. Grossweiner, W.A. Mulac, Rad. Res. 10 (1959) 515.
[52] C.D. Cook, R.C. Woodworth, J. Am. Chem. Soc. 75 (1953) 6242.
[53] C.D. Cook, C.B. Depathi, E.S. English, J. Org. Chem. 24 (1959) 1356.
[54] E. Müller, K. Ley, Chem. Ber. 87 (1954) 922.
[55] A. Abragram, B. Bleaney, Electron Paramagnetic Resonance of Transition Metal Ions, Dover Publication. Inc., New York, 1986.
[56] J. Müller, T. Weyhermüller, E. Bill, P. Hildebrandt, L. Ould-Moussa, T. Glaser, K. Wieghardt, Angew. Chem., Int. Ed. 37 (1998) 616.